Force Generation in the Outer Hair Cell of the Cochlea

K. H. Iwasa and M. Adachi
Biophysics Section, LCB, National Institute of Deafness and Other Communication Disorders, National Institutes of Health, Bethesda, Maryland 20892-0922 USA

ABSTRACT The outer hair cell of the mammalian cochlea has a unique motility directly dependent on the membrane potential. Examination of the force generated by the cell is an important step in clarifying the detailed mechanism as well as the biological importance of this motility. We performed a series of experiments to measure force in which an elastic probe was attached to the cell near the cuticular plate and the cell was driven with voltage pulses delivered from a patch pipette under whole-cell voltage clamp. The axial stiffness was also determined with the same cell by stretching it with the patch pipette. The isometric force generated by the cell is around 0.1 nN/mV, somewhat smaller than 0.15 nN/mV, predicted by an area motor model based on mechanical isotropy, but larger than in earlier reports in which the membrane potential was not controlled. The axial stiffness obtained, however, was, on average, 510 nN per unit strain, about half of the value expected from the mechanical isotropy of the membrane. We extended the area motor theory incorporating mechanical orthotropy to accommodate the axial stiffness determined. The force expected from the orthotropic model was within experimental uncertainties.

INTRODUCTION

The outer hair cell (OHC) is one of the mechanosensory cells in the cochlea. In addition to the sensory function, it has a motility that follows the membrane potential very closely (Brownell et al., 1985; Ashmore, 1987; Santos-Sacchi and Dilger, 1988; Iwasa and Kachar, 1989; Dallos et al., 1991). This motility, which is sometimes referred to as the electromotility, is unique in that it is neither dependent on chemical energy such as ATP (Kachar et al., 1986; Holley and Ashmore, 1988b) nor sensitive to Ca^{2+} (Iwasa et al., 1995). In association with the Deiters' cell, the OHC links the basilar membrane and the reticular lamina. Because of this location, this cell is capable of changing the separation of these two structures and thereby modifying their vibrations in response to acoustic stimulation. Indeed, application of oscillating voltage waveforms across the cochlear partitions induces vibrations of the inner ear through the OHC (Xue et al., 1993; Mammano and Ashmore, 1993). These observations illuminate underlying mechanisms involving the OHC in fine tuning and for the wide dynamic range of the mammalian ear (Mountain, 1980; Lieberman and Dodds, 1984; de Boer, 1991). To perform this function, the force generated by the OHC is expected to be critically important. In this report an elastic probe was used to determine the force generated by the OHC under voltage clamp.

Earlier reports on direct measurements of the motile force were performed in configurations in which a glass electrode, either a smaller suction electrode or a larger microchamber electrode, held the cell at the basal end and a probe applied force to the cuticular plate in the direction of compressing the cell (Hallworth, 1995; Hemmert et al., 1997). In this configuration, voltage pulses were applied across the part of the external surface of the membrane in contact with an electrode. Thus the amplitude of the voltage pulses applied across the cell membrane should depend on the ratio of the electrical impedance of the membrane area in contact with the electrode to the impedance of the rest of the membrane. Thus this quantity could only be estimated. In addition, in these experiments the membrane potential was not controlled, i.e. the effect of possible DC shifts, for example, cannot easily be isolated. In our experiment, we use a patch pipette in the whole-cell recording configuration to control the membrane potential. Thus the membrane potential and the pulse amplitudes are imposed rather than estimated.

Measuring the force produced is not only important for understanding the biological role of the OHC in the cochlea; it also provides us with an important test for examining models for the force generation mechanism in the cell. The OHC has an unusual membrane capacitance that is dependent on the membrane potential (Ashmore, 1990; Santos-Sacchi, 1991; Iwasa, 1993). This capacitance is also dependent on membrane tension (Iwasa, 1993; Gale and Ashmore, 1995; Kakehata and Santos-Sacchi, 1995). Based on these observations, it has been shown that this motility is driven by a membrane motor based on a direct electromechanical coupling (Iwasa, 1993, 1994). The membrane motor has at least two states, and transitions between the states are characterized by a charge transfer across the membrane and mechanical displacement of the motor. The unit of the charge transferred is $\sim 0.8e$ (e is the electronic charge), and the difference in the membrane area of the motor is ~ 3–4 nm^2. By combining the two-state model for the membrane motor and isotropic membrane elasticity determined by a stress-strain relationship during pressure application (Iwasa

Received for publication 2 December 1996 and in final form 25 March 1997.

Address reprint requests to Dr. Kuni H. Iwasa, Biophysics Section, NIDCD, National Institutes of Health, Bldg. 9, Rm. 1E120, 9 Center Dr., MSC 0922, Bethesda, MD 20892. Tel.: 301-496-3987; Fax: 301-480-0827; E-mail: kiwasa@helix.nih.gov.

0006-3495/97/07/546/10 $2.00

and Chadwick, 1992), it was possible to describe the motility of the OHC and predict the force produced under isometric conditions (Iwasa, 1994). By directly measuring the force produced by the cell, this model can be tested.

The isometric force obtained in the present experiment is ~30% less than the value predicted by the previous theory (Iwasa, 1994). The axial stiffness determined in our experiment is, however, about half the value expected from the previous estimate based on a stress-strain relationship during pressure application and a mechanical isotropy. For this reason, we reformulated the previous treatment, introducing mechanical orthotropy (Tolomeo and Steele, 1995). We found that the incorporation of orthotropy into the area motor model gives improved predictions of the force produced by the OHC.

METHODS

Cell preparation

Bullas were obtained from guinea pigs. The organ of Corti was dissociated from opened cochleas by teasing with a fine needle under a dissection microscope. The strips of organ of Corti thus obtained were tritulated three times gently with a plastic pipette and placed in a chamber mounted on an inverted microscope. Clusters of OHCs, preferably formed by two or three cells, connected at their apical end were chosen for experiments.

Probe

Glass capillaries (1.5 mm O.D.) were pulled with a BB.CH.PC puller (Mechanex, Switzerland) to form fine fibers near the tip. These glass capillaries were used as probes after their bending stiffness at the tip was calibrated. The calibration procedure involves bending a probe near the tip by a glass fiber with known stiffness under a microscope. As the primary standard, a relatively long and thick glass fiber was pulled by hand and cut to make a piece 5 cm long. After fixing one end of the thick fiber to a glass capillary with epoxy glue, its bending stiffness at the other end was determined by measuring the displacement under a microscope while a number of thin short platinum wires with known mass (between 0.1 mg and 1 mg) were hung near the tip. To facilitate calibrating the probes used for the experiments, a secondary standard with smaller diameter was used. This procedure was similar to the method described by Kojima et al. (1994). The fiber probes used had stiffness values between 2.5 mN/m and 4.6 mN/m.

Patch clamping

Patch pipettes were fabricated by pulling glass capillaries (blue tip) with a BB.CH.PC puller. Their resistance was between 2 and 3 MΩ when filled with an intracellular medium. The internal medium contained 145 mM KCl, 2 mM $MgCl_2$, 1 mM EGTA, 0.555 mM $CaCl_2$, and 10 mM HEPES. The external medium contained 135 mM NaCl, 5 mM KCl, 2 mM $MgCl_2$, 1.5 mM $CaCl_2$, 5 mM glucose, and 10 mM HEPES. The pH of both media was adjusted to 7.4. A patch amplifier (EPC-7; List Electronic, Darmstadt, Germany) was used for whole-cell voltage clamp experiments. A train of voltage pulses was generated with an ITC-16 interface (Instrutech, Great Neck, NY) on a computer using the Synapse program (Synergistic Research, Silver Spring, MD).

Determination of stiffness

A fiber probe was placed at an extension of the cuticular plate connecting two or three outer hair cells. The cuticular plates of these cells were connected with the phalanx, the rigid apical part of the phalangeal process, of the Deiters' cells. The probe must be placed slightly basal to the connecting structure so that the cell can be pulled (Fig. 1). No part of the outer hair cell was pushed down by the probe. A tight seal was then formed with a patch pipette on one of the cells at the lateral wall near the basal end, but more apical than the nucleus. The system was brought to whole-cell configuration by applying a train of brief pulses across the electrodes (zapping). External tension was applied to the cell by stretching it with the patch pipette while holding the other end with the fiber probe (Fig. 1).

To mark fixed positions on the cell membrane, polyacrolein microspheres 1 μm in diameter (Polysciences, Warrington, PA) were introduced to the external bath in a manner described by Zajic and Schacht (1991). Briefly, 5 μl of microspheres was prediluted into 1 ml of the bath medium, and then 40 μl of the suspension was added to the chamber containing the 200 μl bath medium. Microspheres attached to the surface of the cell were used for determining the axial strain of the cell.

Images of the cell with the fiber probe were stored with a video recorder and digitized off-line with an image grabber card (Scion, Frederick, MD) using a computer program (NIH Image, W. Rasband, NIMH). The accuracy in determining the position of the probe and the axial strain of the cell was enhanced by fitting the light intensity peaks that corresponded to the probe, microspheres, and cell edges with a parabola. The number of points used for the fit was usually five. The process was automated by developing a macro for the NIH Image program.

Movement under an elastic load

In the same configuration as was used for determining the axial stiffness, voltage pulses were delivered to the cell from the patch electrode. To ensure that the OHC is kept under tension, the holding membrane potential was usually set at −80 mV or at a slightly more negative value (See Results). Voltage pulses applied were between 100 ms and 1 s in duration, to be compatible with the video rate. The microscope images of the cell and the probe were stored with a video recorder and analyzed off-line in a manner similar to the stiffness determination described above.

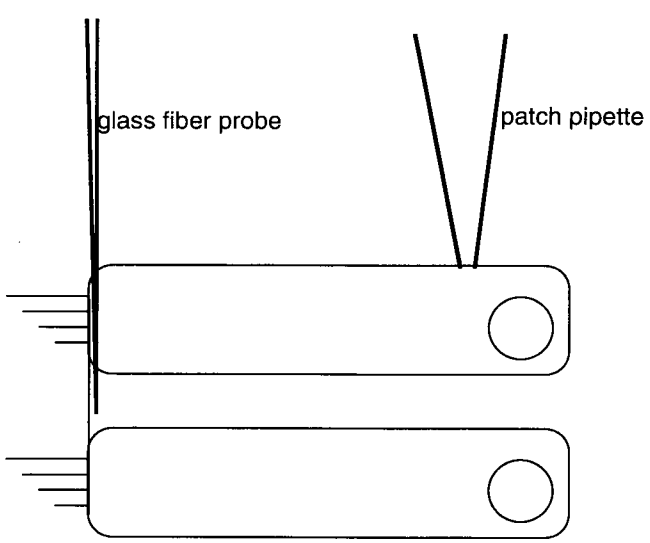

FIGURE 1 Schematic diagram showing the experimental configuration using a fiber probe and a patch pipette for observing the force production. The axes of both patch pipette and the fiber probe are directed downward, making about a 45° angle with the bottom plane of the chamber. The patch pipette is brought into the whole-cell recording configuration. The fiber probe is in contact with the cell at a part of the cuticular plate connecting two cells. To minimize the effect of static friction between the cells and the bottom of the chamber, clusters of the cells that consist of only two or three outer hair cells were selected for the experiment.

RESULTS

Axial stiffness of the cell

Cells were held with the fiber probe at one end and pulled with the patch electrode. The elongation of the cell was not adequately represented by the distance between the fiber probe and the patch pipette. That was because the patch pipette tended to slip on the cell membrane. This slippage was particularly pronounced when the pipette had a tight seal with the cell. This sliding took place while a tight seal was maintained. The cells could be appreciably elongated (more than 10%) only when the pipette did not form a tight seal. (This observation appears to suggest that a tight seal is formed only when the membrane is pulled away from underlying cytoskeleton.) For this reason, the elongation of the cell was determined by measuring the distance between the cuticular plate and a microsphere attached to the lateral membrane. Instead of a microsphere, an identifiable structure, usually a mitochondrion, near the lateral wall could also be used. The choice between these two markers did not make a significant difference in evaluating the axial strain.

The axial stiffness of the cell was characterized by the ratio of axial force F_z, which was determined by the bending of the fiber probe, to the axial strain ϵ_z of the cell (Fig. 2). We used the ratio F_z/ϵ_z, which we refer to as the "axial stiffness," for describing the axial elasticity of the cell. The data points in the plot were taken at 1-s intervals. In some experiments the sampling interval was 0.2 s. The mean value for the stiffness was 512 nN, and the standard deviation was 103 nN (Table 1). The values given in the table were taken at −80 mV holding potential. The values for the stiffness ranged between 700 nN and 300 nN and did not show a clear dependence on the cell length, which ranged from 30 μm to 85 μm (Fig. 3).

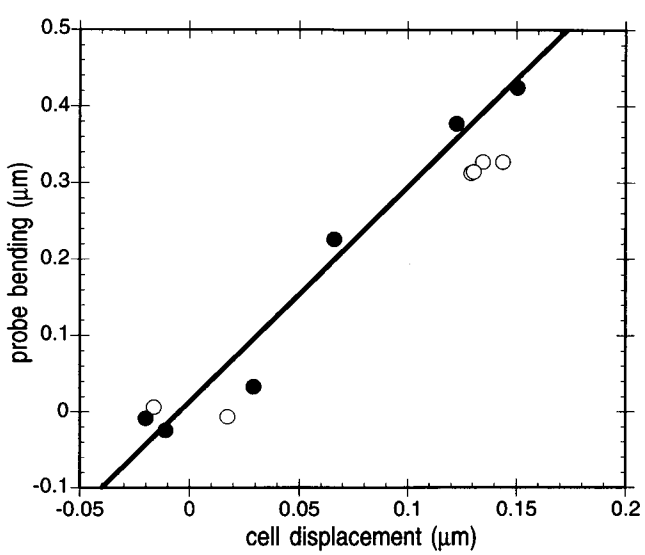

FIGURE 2 Probe bending plotted against cell displacement to determine the stiffness of the cell. The patch pipette was moved away from the probe to apply tension to the OHC. The force applied to the cell was determined from the bending of the fiber probe, which has a stiffness (k_p) of 2.8 mN/m. The length change of the cell was determined by using microspheres attached to the cell surface. At zero displacement, the distance L was 44 μm. Two stretches of the same cell are plotted. The membrane potential was −80 mV. A fit (*solid line*) gives $\Delta z_p/\Delta z_c = 2.9 \pm 0.2$. The force balance is represented by $k_p\Delta z_p = K_c\Delta z_c/L$. This gives (357 ± 25) nN for the axial stiffness K_c of the cell.

Measuring the stiffness of the cell at a holding potential far from the reversal potential was difficult. At a more negative holding potential such as −90 mV, the cell tended to shorten. At a more positive holding potential, the cells became flattened and the probe tended to lose firm contact with the cell. This observation seems to be associated with cellular electrolyte gain or loss during voltage clamp. A voltage clamp condition imposes a steady membrane current if the holding potential is not exactly the same as the reversal potential. The steady electric current at the junction between the cell and the patch pipette must be equal to the current through the rest of the membrane. However, the membrane has a selectivity, whereas there is no selectivity at the cell-pipette junction. Thus ionic flows at these two places are different, resulting in a gain or loss of cellular volume quantitatively consistent with the observation (Iwasa, 1996).

Cell movement with an elastic load

The experimental configuration for measuring the axial stiffness was also used for monitoring cell motion with an elastic load. To maintain adequate contact between the cell and the probe, the membrane potential was held around −80 mV. The patch pipette was used for both clamping the membrane potential and holding the cell at its basal end. Bending of the probe elicited by depolarizing voltage pulses was measured. In Fig. 4 responses to long pulses (1-s duration) are shown. In most cases the responses to square pulses of this duration did not show a significant creep. Reliable measurements of the displacement amplitude required a minimum pulse duration of 150 ms. The dependence of the bending amplitude on the pulse amplitude is shown in Fig. 5. Because the bending of the probe did not show a significant deviation from a linear dependence on the membrane potential in the interval between −80 mV and +20 mV, we summarized the data using the mean slope (Table 1). Pulses were not applied in the hyperpolarizing direction because elongating forces could not be reliably applied to the probe in our experimental configuration. During pulses the patch pipette did not slide along the cell. The force thus obtained from the bending of the probe is dependent not only on the properties of the cell, but also on the stiffness of the probe (Table 1). This is because a force balance is established when the probe's elastic force is equal to the motile force of the cell. Because the force produced by the cell decreases as the cell deforms, and because a more compliant probe requires a larger bending than a stiffer probe does to produce a given force, the force at the equilibrium is smaller when the probe is more compliant.

TABLE 1 Probes used and values for cell stiffness, bending of the probe, and isometric force obtained

Probe stiffness k_p (mN/m)	Cell's axial stiffness (nN)	Probe bending (nm/mV)	Force at the probe (nN/mV)	Isometric force est. (nN/mV)	n
2.5	501 ± 132	6.16 ± 2.65	0.015 ± 0.007	0.091 ± 0.025	10
2.8	559 ± 91	7.95 ± 1.95	0.022 ± 0.005	0.116 ± 0.031	4
4.6	502 ± 63	6.75 ± 2.03	0.031 ± 0.009	0.104 ± 0.047	8
Total	512 ± 103			0.100 ± 0.035	22

The standard deviations are given after the mean values. The force at the probe is obtained with $\Delta z_p k_p$, where Δz_p is probe bending and k_p is probe stiffness. It shows a correlation with the stiffness of the probe. The estimates for isometric force are obtained with the formula $(k_p + K_c/L)\Delta z_p$, which is equivalent to $(K_p + K_c)\varepsilon_z$. Here K_c is the axial stiffness of the cell and L represents the separation between the fiber probe and the patch pipette. The theoretical justification of the formula is given in the Appendix (Eq. A7).

The force independent of the probe stiffness is obtained as the isometric force, which is an extrapolation to infinite probe stiffness. This extrapolation (Fig. 6) is approximately obtained by multiplying the bending of the probe by the sum of elastic coefficients for the probe and the cell (Table 1), as described in the Appendix.

The isometric force elicited by voltage pulses showed some correlation with the cell length (Fig. 7). The result seems to indicate that longer cells tend to produce force more effectively than shorter cells, although the correlation is relatively low.

DISCUSSION

The axial stiffness of the cell

The axial stiffness (512 ± 103 nN per unit strain) of the OHC that we obtained in the present work is relatively larger and more uniform compared with the values reported by Hallworth (1995). His mean value is around 200 nN, and his upper bound is around 750 nN. The values we obtained lie between his mean value and upper bound. The values obtained by Holley and Ashmore (1988a) are much smaller, ~40 nN on average. We have no reason to believe that our method overestimates the stiffness, and we can suggest possible reasons why our values are larger than previously reported estimates.

The factor most likely to affect our measurement is friction between the cell and the bottom of the chamber. Because friction reduces the movement of the fiber probe, this factor can only reduce our estimate for the stiffness. Thus this factor cannot lead to overestimation of the stiffness.

The difference could be related to the experimental configurations. Whereas the earlier reports are obtained from compression experiments, the values we obtained are based on elongation experiments. A possible reason that we obtained values higher than previous reports is that a compression may result in a bending of the cell but an extension does not. It is also possible that an elastic force due to compression is more sensitive to the turgor pressure than an elastic force for extension.

Another factor that may contribute to the difference is dialysis of the cytoplasm during the whole-cell mode. Our data were obtained within 1 min of forming the whole-cell mode. Prolonged monitoring beyond 1 min tended to reduce

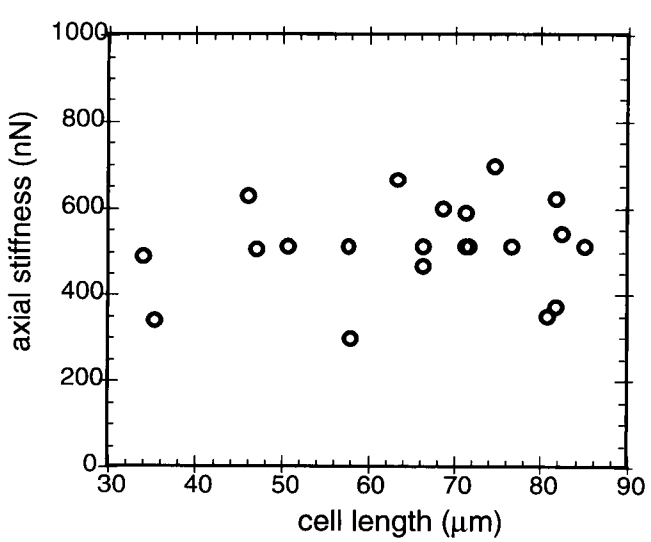

FIGURE 3 The axial stiffness plotted against the cell length. The axial stiffness is defined as the axial elastic force per unit axial strain.

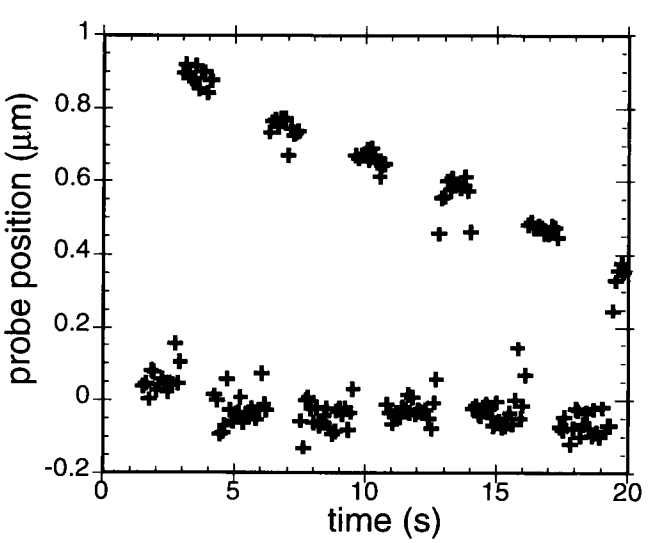

FIGURE 4 Bending of an elastic probe by the OHC under voltage clamp. The bending of the probe is plotted against time. The holding membrane potential is −80 mV. Data points are taken every 62.5 ms. The duration of the pulses is 1 s. The amplitude of the depolarizing pulses starts from 100 mV (*left*), and it is reduced by 10 mV at each successive pulse.

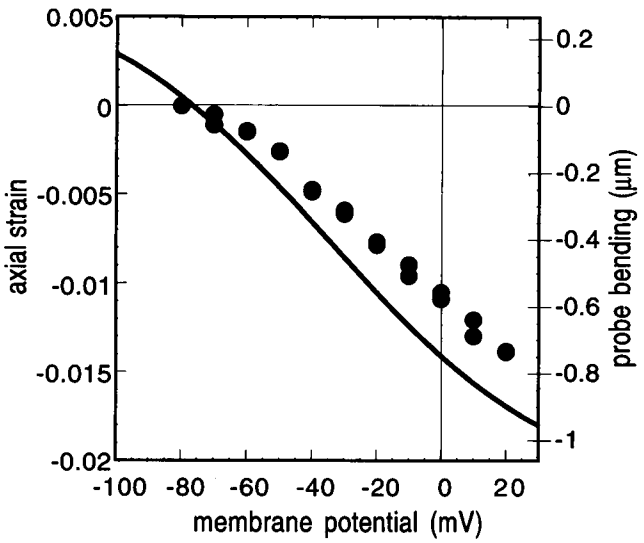

FIGURE 5 Bending of an elastic probe by the OHC under voltage clamp. The bending Δz_p of the probe is plotted against the pulse amplitude (*filled circles*). The bending (*right ordinate label*) of the probe is related to the axial strain ϵ_z (*left ordinate label*) of the cell ($\epsilon_z = \Delta z_p/L$). The holding potential is −80 mV. The stiffness of the fiber probe is 2.8 mN/m, and the axial stiffness of the cell is 695 nN. The solid line is based on the theoretical model using parameter values given in the legend to Fig. 9, except for the elastic moduli of the cell. A set (d_z, d_c, c) = (54 mN/m, 64 mN/m, 48 mN/m) is consistent with the stress-strain relationship ($\epsilon_z/P = -6.9 \times 10^{-5}$, $\epsilon_c/P = 1.3 \times 10^{-4}$ Pa^{-1}) for pressure application (Iwasa and Chadwick, 1992) and gives the right axial stiffness (paresent experiment). See the Appendix for details.

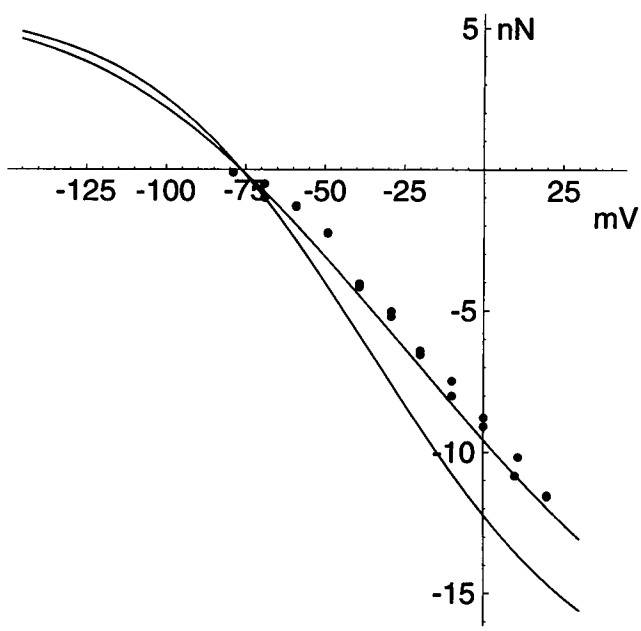

FIGURE 6 Isometric force plotted against the membrane potential. Isometric force was obtained by Eq. A6, using the probe stiffness, the axial stiffness, the distance between the probe and the patch pipette, and the bending amplitude of the probe (*filled circles*). The data set is the same as in Fig. 5. The less steep solid line represents the isometric force based on the theoretical model with the same parameter values as in Fig. 5. The slope is 0.12 nN/mV. The steeper solid line was obtained by using Eq. A7 (the "tension insensitive" approximation) on the theoretical values shown in Fig. 5. The slope is 0.15 nN/mV. The difference between the two solid lines indicates errors created by using Eq. 7.

the cell stiffness. Because our values for the stiffness are larger, this effect is unlikely to have contributed to the difference.

The other factor that may explain a larger variability and smaller values for the stiffness is mechanical inhomogeneity of the cell. We found that the axial strain of the basal membrane was severalfold larger than the lateral wall when the cell was held at both ends. This inhomogeneity has the effect of lowering the stiffness for the entire cell if the cell is held at the synaptic end, as in some of the previous reports (Hallworth, 1995). The lower stiffness at the synaptic end does not appear to have a biological importance because the cell is held near the nucleus by the Deiters' cup. For this reason we held the cell with a patch pipette above the nucleus.

Force generation by the OHC

The quantity we measured was the bending of the elastic probes, which can depend on various factors, which include probe stiffness, cell length, and cell stiffness, as we have described earlier. These experimental data can be directly compared with theoretical predictions (Fig. 5). However, it is more convenient to extrapolate the force that would be measured by a probe of infinite stiffness. The dependence on various parameters disappears in this limit. For convenience, we call this condition the isometric limit and the force obtained in this limit the isometric force.

To obtain the isometric force we can use a simple approximate formula. If we assume that the cell volume is kept constant, we can replace the cell with a series combination

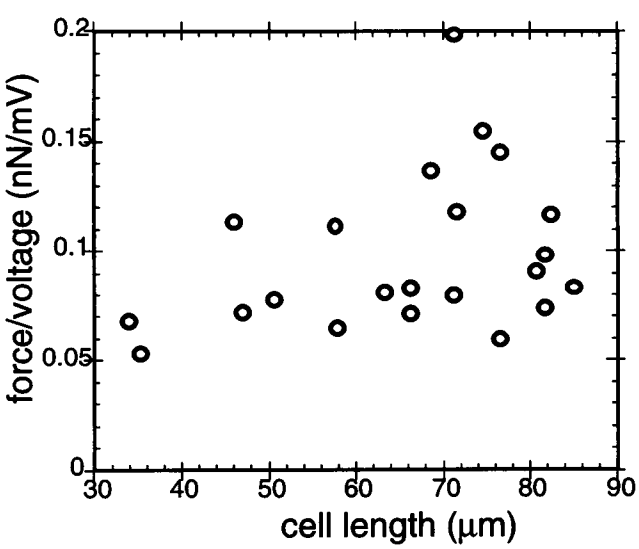

FIGURE 7 The sensitivity of isometric force to voltage changes plotted against the cell length.

of a simple one-dimensional spring with a displacement motor (Fig. 8 *B*). The system can be described easily if the displacement motor is not sensitive to an axial force. The isometric force is given by $(k_p + k_c)\Delta z_p$, where k_p and k_c are stiffnesses of the probe and the cell, respectively, and Δz_p is the displacement of the probe. In the Appendix we show that it is a good approximation of the two-dimensional area motor model (Iwasa, 1994, 1996, 1997). An example of isometric force is shown in Fig. 6.

The formula can be tested directly by using fiber probes that differ in stiffness. The formula is correct if agreement is obtained between the estimates for the isometric force based on data obtained with probes with different stiffness values. Indeed, the sensitivity of the isometric force to the membrane potential is independent of the stiffness of the probes used, and it is around 0.1 nN/mV (Table 1).

A previous report by Hallworth (1995) is more variable. His mean value is 20 pN/mV and his highest value is 70 pN/mV. Thus the value obtained in our experiment is close to the upper end of his range. A report by Hemmert et al. (1997) appears to give values somewhat larger than Hallworth's. There are two important differences between the present experiment and earlier ones. One of them is that our experiment is performed under voltage clamp. That is, unlike earlier reports, the pulse amplitudes in our experiment are known and not estimated. In addition, in our experiment there is no effect of DC voltage shift by stimulation, unlike earlier experiments. The other difference is that we have measured the shortening force, whereas the elongating force was described in earlier reports. Here we do not have a reason to believe our method gives an overestimate of the force production. The friction between the chamber and cell reduces the amplitude measured at the probe in our configuration, leading to an underestimate of the force. In the configuration reported previously, various factors, including a bending of the cell, may lead to underestimates of the force. If the cell is held at the very end of the synaptic side, a lower stiffness of the cell in the synaptic region also lowers the force production. These factors are similar to the ones considered in the discussion on the determination of the axial stiffness.

Comparison with theoretical models

Our experimental value of 0.1 nN/mV for isometric force production is somewhat smaller than the value 0.15 nN/mV predicted by the area motor model (Iwasa, 1994) based on mechanical isotropy, in which elastic moduli were determined from the strain-stress relationship during pressure application (Iwasa and Chadwick, 1992). The axial stiffness predicted by that isotropic membrane model, however, is 1000 nN, larger than the value we obtained in this report by a factor of 2. Although this factor is not very large, it exceeds experimental uncertainties. To address this issue, we incorporated mechanical orthotropy into the area motor model (Appendix). In an orthotropic model the elastic modulus d_z relating the axial stress and the axial strain is different from the elastic modulus d_c relating the circumferential stress and the circumferential strain. For this reason, the elastic coefficients are chosen to satisfy two relationships, the stress-strain relationship during pressure application (previously measured) and the axial stiffness determined in the present experiment. Details of the determination are given in the Appendix. The mean values are 43 mN/m for d_z, 61 mN/m for d_c, and 42 mN/m for the cross-modulus c.

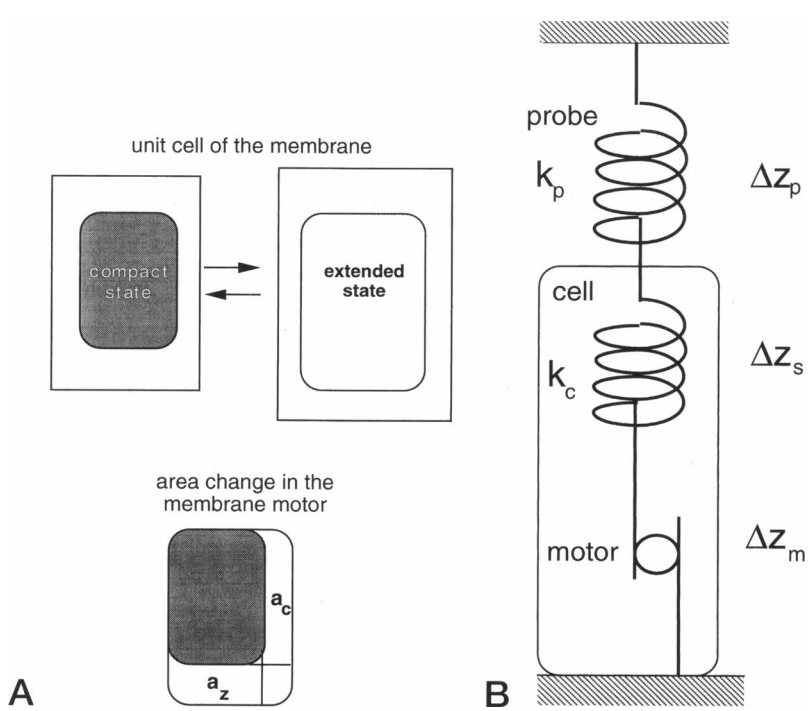

FIGURE 8 (*A*) Schematic diagram representing conformational changes of the membrane motor. The up-down direction corresponds to the axial direction of the OHC. The conformational transition changes the unit cell of the membrane. This effect is expressed in terms of membrane strains by $\epsilon_z = \epsilon_z' + nP_1a_z$ and $\epsilon_c = \epsilon_c' + nP_1a_c$ (see text). (*B*) Schematic diagram of the system in which the OHC is approximated by a series combination of a spring and a displacement motor. The displacement Δz_p of the probe spring gives rise to an elastic force $k_p\Delta z_p$, which is equal to $k_c\Delta z_s$ due to the elastic force of the spring in the cell. In this system, the length relationship $\Delta z_p + \Delta z_s + \Delta z_m = 0$ should hold, where Δz_m is motor displacement. Elimination of Δz_s from these two equations yields $(k_p + k_c)\Delta z_p = -k_c\Delta z_m$. An isometric condition can be realized as the limit $k_p \to \infty$. Under this condition the displacement of the probe is null and $\Delta z_s = -\Delta z_m$. The isometric force $k_c\Delta z_s$ in the isometric condition is represented by $-k_c\Delta z_m$. If motor displacements are determined by the membrane potential alone, the motor displacement with an elastic load is the same as that under the isometric condition. Thus the isometric force is expressed by $(k_p + k_c)\Delta z_p$, which is equivalent to the quantity $(K_p + K_c)\epsilon_c$ in the Appendix.

The basic assumptions for the previous isotropic model were that 1) the shape of the cell can be approximated by a cylinder, which is supported by the lateral membrane; 2) the motor has two states that differ in charge and cross-sectional area in the membrane; 3) the membrane is purely elastic, and the elastic property of the motor is the same as that of the rest of the membrane; 4) the mechanical strains are expressed as a sum of motor strains and elastic strains; and (5) there is mechanical isotropy of the lateral membrane. These assumptions were intended to minimize the number of parameters. Because we found that mechanical isotropy, which requires the least number of parameters, is incorrect, we use mechanical orthotropy, which requires one more parameter than isotropy, together with the four other assumptions (Appendix). In the previous paper (Iwasa, 1994), assumptions 2) and 4) were illustrated by a picture in which the motor floats in the plasma membrane. Although this picture is the simplest to illustrate, it contradicts the observation that the measured stiffness of the membrane is less than that of a lipid bilayer. In the present work, we found that the membrane is more compliant in the axial direction, a factor further incompatible with a lipid bilayer. For this reason the motor unit must include cytoskeletal elements, and the change in the motor area can be interpreted as the effective area change in the cytoskeleton together with the plasma membrane. This interpretation could be challenged by the observation that the electromotility of the OHC in the load-free condition persists, even after internal digestion of the cell by trypsin (Kalinec et al., 1992; Huang and Santos-Sacchi, 1994). This observation, however, may not contradict the importance of cytoskeleton in force production. It is likely that trypsin digestion of the cytoskeleton would make the cell membrane flaccid and soft, so that not much force is required to move the membrane after digestion.

The area motor model based on mechanical orthotropy with the experimentally determined axial stiffness predicts ~0.10 nN/mV for force production (Fig. 9 *A*). This is about the same as the average value 0.100 ± 0.035 nN/mV for force production estimated from our experiment (Table 1). However, this comparison is not quite accurate. The procedure used for extrapolating the data obtained with the probes used (with a stiffness between 2.5 and 4.6 mN/m) is based on an approximate formula (Eq. A7 in the Appendix) and may lead to some errors. Our simulation, based on the membrane motor model, shows that this extrapolation leads to estimates ~20% larger than the true values of isometric force (Figs. 6 and 9 *A*). Nonetheless, these errors are within the experimental uncertainties, and thus the agreement between the theory and the experimental data remains reasonable. Besides, this agreement is obtained without an adjust-

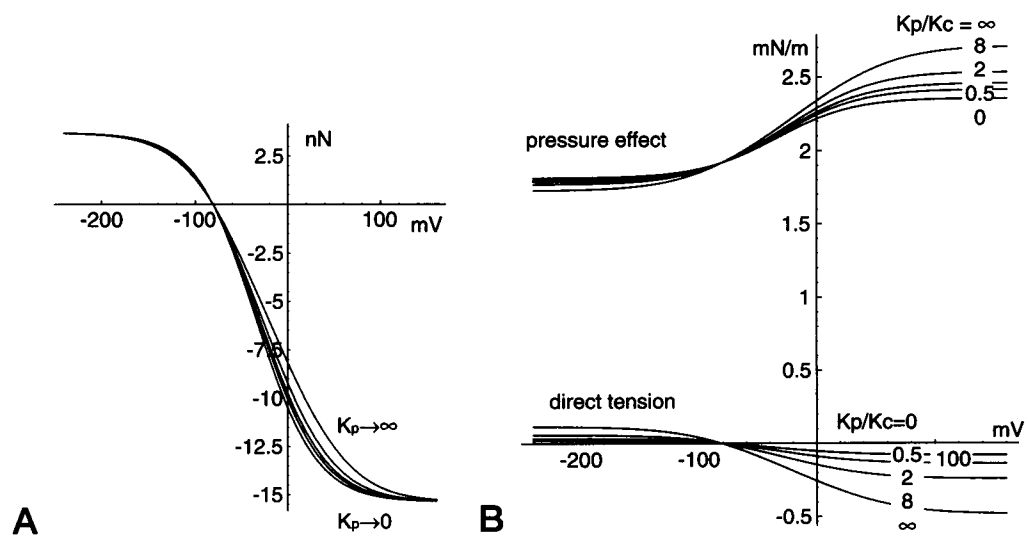

FIGURE 9 Behavior of the OHC under an elastic load as predicted by the area motor model. An orthotropic elasticity is assumed for the cell. Values used: $0.8e$ for the unit moving charge q, $3.7 \times 10^3/\mu m^2$ for the number density n of the membrane motor, 5 μm for the radius r of the cell, 8 nm^2 for the area change a_z of the motor in the axial direction during a transition from the compact state to the extended state, -1.5 nm^2 for area change a_c in the circumferential direction during the transition. These values are similar to the previous paper (Iwasa, 1994). The volume strain ϵ_{v0} of the reference state is chosen to be 0.08, which corresponds to a turgor pressure of 0.47 kPa. The value 2.4 is chosen for the constant F_0/kT in the free energy difference to adjust the voltage of the maximum slope. The values for the elastic moduli used are d_z = 46 mN/m, d_c = 68 mN/m, and c = 46 mN/m. This set is chosen to give 500 nN for the axial stiffness of the cell and to satisfy the stress-strain relationship during pressure application (Iwasa and Chadwick, 1992). (*A*) The quantity $\epsilon_z(K_p + K_c)$ plotted against the membrane potential. The axial strain ϵ_z under various values of elastic load K_p is calculated, and then the product $\epsilon_z(K_p + K_c)$ is plotted against the membrane potential. Although changes are not large, with a stiffer probe the transition is sharper and the midpoint potential shifts in the hyperpolarizing direction. The traces correspond to K_p/K_c = 0, 0.5, 2, 8, and infinity. Our experimental condition is close to K_p/K_c = 0.5. The mean slope between −80 mV and 20 mV for this trace is 0.12 nN/mV. The mean slope for the interval for the true isometric condition is 0.10 nN/mV. This gives an error estimate of 20%. The difference in the slope from Fig. 6 is due to different values for the axial stiffness of the cell. (*B*) An axial tension T_{xl} (*bottom traces*) exerted by the fiber probe and the contribution $rP/2$ of the intracellular pressure (*top traces*) plotted against the membrane potential. These quantities undergo changes while the OHC with an elastic load is driven by voltage pulses. The conditions K_p/K_c = 0, 0.5, 2, 8, and infinity, respectively, correspond, from the top trace to the bottom, to T_{xl} and, from the bottom trace to the top, to rP.

able parameter. Three elastic moduli are determined by the pressure response of the cell (Iwasa and Chadwick, 1992) and the measured axial stiffness. The number of the motor in the cell, the charge transferred across the membrane, and area change during conformational transitions of the motor must be consistent with capacitance measurements (Iwasa, 1993). The ratio of area changes in the two directions must satisfy the saturating amplitude of ~4% in the load-free condition. These conditions do not leave any adjustable parameters.

There are, however, a number of differences between the experimental configuration and the conditions assumed for the calculation. Perhaps the most significant difference is how the cell is held. In the experiment, the cell was held at the cuticular plate with a fiber probe and at the lateral wall somewhat above the nucleus with a patch pipette. In the model calculation, external axial force is applied end to end. This difference should result in reduced changes in the internal pressure in our experiment compared with the theory, because a part of the cell membrane is not subjected to the externally applied constraint. Indeed, the weak correlation between the efficiency of force production and cell length (Fig. 7) could be an artifact due to this pressure factor, because the fraction of the synaptic region, which is not included in the model, is larger for shorter hair cells. For this reason, our theoretical model is expected to provide a better description of longer cells.

Despite these reservations, we could conclude that the agreement between the theory and the experiment is rather satisfactory. Our model is rather static, however. Some of the assumptions, which appear to be adequate for a static description, may need a reexamination for extending the model to describe the behavior of the cell at the auditory frequencies. For example, the assumption of homogenized strain (i.e., assumption 4) may not be valid for describing the behavior of the cell in this frequency range. It is possible that the membrane motor undergoes very fast transitions, but the "homogenization" of the strains in its vicinity may require a certain relaxation time after the transition. This effect might account for the increased force production observed at higher frequencies (Hemmert et al., 1997).

We used a two-state model for the membrane motor in this treatment. The validity of our argument is, however, not limited to this particular model. The relative insensitivity of the membrane area motor to an axial elastic load is equally applicable to a multistate model as well as the two-state model. Because a three-state model, for example, can predict a membrane potential dependence that is practically indistinguishable from that of the two-state model we used (Iwasa, 1996), the three-state model is expected to agree with the experimental data as well as the two-state model we used.

APPENDIX: ORTHOTROPIC TWO-DIMENSIONAL MODEL

Here the area motor model (Iwasa, 1994, 1996) for the electromotility of the OHC is extended by incorporating mechanical orthotropy instead of mechanical isotropy. In addition, we show that the membrane motor, paradoxically, is not very sensitive to an externally applied axial tension and provide a simpler description of the cell, assuming the membrane motor is tension insensitive. We also give an estimate of errors due to the "tension-insensitive" approximation.

The OHC is approximated by a cylinder of length L and radius r. We also assume that the OHC is elastic. This assumption is expected to be adequate for describing displacements of the cell for durations not exceeding several seconds (Ehrenstein and Iwasa, 1996). Tension T_z in the axial direction and tension T_c in the circumferential direction due to elastic strains ϵ_z' (axial direction) and ϵ_c' (circumferential direction) are balanced by the force due to internal pressure p and an axial tension T_{xt} due to a force externally applied in the axial direction,

$$d_z\epsilon_z' + c\epsilon_c' = T_z = \frac{1}{2}rp + T_{xt},$$
$$c\epsilon_z' + d_c\epsilon_c' = T_c = rp \tag{A1}$$

where d_z is a diagonal element of the elastic tensor relating an axial stress to an axial strain ϵ_z', d_c is another diagonal element related to the strain ϵ_c' in the circumferential direction, and c is the off-diagonal element. Equation A1 is based on a mechanical orthotropy that was first proposed for the OHC by Tolomeo and Steele (1995). Isotropy is a special case of orthotropy in which both diagonal components are equal, and these elastic constants are represented by an area modulus K and a shear modulus μ. Namely, $d_z = d_c = K + \mu$ and $c = K - \mu$. As in a previous treatment (Iwasa, 1994), we assume that the total strains ϵ_z and ϵ_z are represented by sums of the elastic strains and motor strains, i.e.,

$$\epsilon_z = \epsilon_z' + nP_1a_z \quad \text{and} \quad \epsilon_c = \epsilon_c' + nP_1a_c \tag{A2}$$

Here n is the (number) density of the motor in the lateral membrane, a_z is the axial component of the area change of the motor, and a_c is the circumferential component (Fig. 8 *A*). The probability that the motor is in the extended state is represented by P_1,

$$\frac{P_1}{1 - P_1} = \exp\left[-\frac{\Delta F}{k_BT}\right], \tag{A3}$$

with the free energy difference of the motor in the two states:

$$\Delta F = F_0 + qV + (a_zT_z + a_cT_c) \tag{A4}$$

where F_0 is a constant, q the charge transferred between the two states, V the membrane potential, k_B the Boltzman constant, and T the temperature.

Eliminating the elastic strains with Eqs. A1 and A2, membrane tensions in the two directions are rewritten as

$$T_z = d_z\epsilon_z + c\epsilon_c + f_zP_1,$$
$$T_c = c\epsilon_z + d_c\epsilon_c + f_cP_1. \tag{A5}$$

Here the constants f_z and f_c are related to these elastic constants and the area difference of the motor in the two states,

$$f_z = -n(d_za_z + ca_c),$$
$$f_c = -n(ca_z + d_ca_c).$$

The externally applied tension due to an elastic load can be represented by

$$T_{xt} = -K_p\epsilon_z, \tag{A6}$$

if the load is connected in series. The minus sign appears because the elongation of the cell is equal to the shortening of the elastic probe. If the elastic force of the probe is $k_p\Delta z$ for a displacement Δz, the elastic constant introduced is represented by $K_p = k_pL/(2\pi r)$, where r and L are, respectively, the radius and the length of the cell. This assumes that the cell is held at the ends.

It is reasonable to assume that the volume of the cell is constant for responses to changes in the membrane potential (Iwasa and Chadwick, 1992). A constant volume condition, $\epsilon_z + 2\epsilon_c = \epsilon_{v0}$, reduces the number of variables, where ϵ_{v0} is the volume strain in the standard membrane potential. With Eqs. A1 and A5 and an elastic load (Eq. A6), the axial strain is given in the form

$$(K_c + K_p)\epsilon_z = a + bP_1, \tag{A7}$$

where constants a, b, and K_c, which is the axial stiffness of the cell, are given by

$$a = -\frac{1}{2}\left(c - \frac{1}{2}d_c\right)\epsilon_{v0},$$

$$b = -\frac{1}{2}(2f_z - f_c), \tag{A8}$$

$$K_c = d_z - c + \frac{1}{4}d_c.$$

Here the probability P_1 of the extended state is dependent on the membrane potential V as well as the stress, as Eqs. A3 and A4 show.

The load-free condition is equivalent to the limit $K_p \to 0$. Thus the load free strain is formally represented by $(a + bP_1)/K_c$. Likewise, isometric tension is the value of $K_p\epsilon_z$ in the limit of $K_p \to \infty$, and it is thus $a + bP_1$. These relationships give a simple description of the cell if the state P_1 of the motor is solely determined by the membrane potential, namely if it is not sensitive to membrane tension. The isometric tension can then be obtained as $(K_p + K_c)\epsilon_z$. These relationships can also be derived for the one-dimensional case by assuming that the cell consists of a spring and a displacement motor connected in series (Fig. 8 *A* and the caption).

Before numerical examinations, we need to determine the parameters used in the model. The axial stiffness, the mean experimental value of which is 510 nN, is represented by $2\pi r K_c$, where the radius r is usually ~5 μm. Although the motor could contribute to the axial stiffness, the effect of the motor in the cellular response to an externally applied axial force is not significant under voltage clamp, as shown below (in "tension insensitive" approximation). Other conditions used to determine the elastic moduli are strains during pressure application. It has been shown previously that $\epsilon_z/P = -6.9 \times 10^{-5}$ and $\epsilon_c/P = 1.3 \times 10^{-4}\text{Pa}^{-1}$ (Iwasa and Chadwick, 1992). Because the linear response to pressure application extends to relatively large strains, where the effect of the motor is not significant, the total strains can be approximated by the elastic strains to determine the elastic moduli, as in the previous treatment (Iwasa, 1994). Thus Eq. A1 provides the conditions for the elastic moduli. From these conditions we obtain the values of the elastic moduli. The average values are $d_z = 43$ mN/m, $d_c = 61$ mN/m, $c = 42$ mN/m. These values satisfy $d_z d_c > c^2$, the condition between the elastic moduli (Iwasa and Chadwick, unpulished). Isotropy is a special case of orthotropy with one less parameter, i.e., $d_z = d_c = K + \mu$ and $c = K - \mu$, and the axial stiffness is represented by $2\pi r \cdot (K + 9\mu)/4$. The previously determined values, $K = 70$ mN/m and $\mu = 7$ mN/m, lead to an axial stiffness of 1000 nN, which is inconsistent with the measured value for the axial stiffness.

The determination of motor parameters has been discussed in the previous papers (Iwasa, 1993, 1994), and we give here a brief description. The membrane potential dependence of the membrane capacitance gives the number of the motor in a cell and the gating charge. The number density of the motor is $\sim 3.7 \times 10^3/\mu\text{m}^2$, and the gating charge q is $0.8e$ (Ashmore, 1990; Santos-Sacchi, 1991; Iwasa, 1993), where e is the electronic charge. The area change of the motor during conformational changes is determined by changes in the membrane capacitance during pressure application, and the estimate we used is ~3.3 nm^2, which theoretically is $2(2a_c + a_z)/3$ (Iwasa, 1993, 1994). Because changes in membrane tension due to pressure application are determined primarily by the geometry of the cell and pressure changes, this estimate is virtually unaffected, regardless of whether we assume mechanical isotropy. The area change in the motor is also consistent with the saturating amplitude of 4% in the load-free condition (Ashmore, 1987; Santos-Sacchi and Dilger, 1988). These conditions lead to approximate values $a_z = 8$ nm^2 and $a_c = -1.5$ nm^2. The free energy difference F_0 between the two conformations is set so that the midpoint of the transition is about -20 mV in the load-free condition, with a resting turgor pressure of ~0.5 kPa.

We attempted to determine whether the isometric tension is approximated by the quantity $(K_p + K_c)\epsilon_z$ numerically. Although the theory contains a number of parameters, these parameters are not adjustable, being determined experimentally. Our numerical examination shows that for the motor area displacements a_z and a_c, which are consistent with experimental data, the isometric tension can be approximated by the quantity $(K_p + K_c)\epsilon_z$. The inverse of the bending of the probe is proportional to the sum $K_p + K_c$ of the two stiffnesses, and the voltage dependence of the quantity $(K_p + K_c)\epsilon_z$ is relatively constant, although small voltage shifts do take place (Fig. 9 *A*).

The insensitivity to tension might appear counterintuitive. The membrane motor is sensitive to membrane tension caused by changes in the internal pressure (Iwasa, 1993; Gale and Ashmore, 1995; Kakehata and Santos-Sacchi, 1995). An externally applied tension could be more effective than pressure because the motor is sensitive to axial tension and because applied pressure increases membrane tension more in the circumferential direction than in the axial direction. The reason for this paradox is partially that a tension directly applied to the cell by a fiber probe is relatively small. For example, a 1-kPa internal pressure applied to the cell produces ~80 nN force in the axial direction. In comparison, the force plotted in Fig. 9 *a* is up to 15 nN. In addition, an externally applied axial tension reduces the internal pressure, which in turn reduces membrane tension (Fig. 9 *B*). Because of these effects, the membrane motor is not very sensitive to an external axial force if the values for a_z and a_c are in the range consistent with experimental data.

If the axial area change a_z of the motor increases out of this range, the load free displacement increases but the isometric force decreases, as in the isotropic case previously studied (Iwasa, 1994). Thus the motor becomes sensitive to the axial tension, reducing the cellular force in the isometric limit. Under this condition, the "tension-insensitive" approximation for the motor breaks down.

The extrapolated isometric force predicted by the model with the given set of parameters is 0.12 nN/mV for the conditions that match our average experimental parameters. This extrapolation method is expected to give an overestimate of the true isometric force by ~20% (Fig. 9 *A*).

Ken Iwasa contributed to the development of the macro used for image analysis. The authors thank Dr. David Mountain for his comments, which were useful in developing the method. Comments by Drs. Gerald Ehrenstein, Richard Chadwick, and David Ehrenstein are also appreciated.

REFERENCES

Ashmore, J. F. 1987. A fast motile response in guinea-pig outer hair cells: the molecular basis of the cochlear amplifier. *J. Physiol. (Lond.).* 388: 323–347.

Ashmore, J. F. 1990. Forward and reverse transduction in guinea-pig outer hair cells: the cellular basis of the cochlear amplifier. *Neurosci. Res. Suppl.* 12:S39–S50.

Brownell, W., C. Bader, D. Bertrand, and Y. Ribaupierre. 1985. Evoked mechanical responses of isolated outer hair cells. *Science.* 227:194–196.

Dallos, P., B. N. Evans, and R. Hallworth. 1991. Nature of the motor element in electrokinetic shape changes of cochlear outer hair cells. *Nature.* 350:155–157.

de Boer, E. 1991. Auditory physics. Physical principles in hearing theory III. *Phys. Rep.* 203:125–231.

Ehrenstein, D., and K. H. Iwasa. 1996. Viscoelastic relaxation in the membrane of the auditory outer hair cell. *Biophys. J.* 71:1087–1094.

Gale, J. E., and J. F. Ashmore. 1995. Charge displacement induced by rapid stretch in the basolateral membrane of the guinea-pig outer hair cell. *Proc. R. Soc. Lond. Biol.* 255:233–249.

Hallworth, R. 1995. Passive compliance and active force generation in the guinea pig outer hair cell. *J. Neurophysiol.* 74:2319–2328.

Hemmert, W., C. Schauz, H.-P. Zenner, and A. W. Gummer. 1997. Force generation and mechanical impedance of outer hair cells. *In* Diversity in Auditory Mechanics. E. R. Lewis, G. R. Long, R. F. Lyon, P. M. Narins, and C. R. Steele, editors. World Scientific, Singapore. In press.

Holley, M. C., and J. F. Ashmore. 1988a. A cytoskeletal spring in cochlear outer hair cells. *Nature.* 335:635–637.

Holley, M. C., and J. F. Ashmore. 1988b. On the mechanism of a high-frequency force generator in outer hair cells isolated from the guinea pig cochlea. *Proc. R. Soc. Lond. Biol.* 232:413–429.

Huang, G., and J. Santos-Sacchi. 1994. Motility voltage sensor of the outer hair cell resides within the lateral plasma membrane. *Proc. Natl. Acad. Sci. USA.* 91:12268–12272.

Iwasa, K. H. 1993. Effect of stress on the membrane capacitance of the auditory outer hair cell. *Biophys J.* 65:492–498.

Iwasa, K. H. 1994. A membrane motor model for the fast motility of the outer hair cell. *J. Acoust. Soc. Am.* 96:2216–2224.

Iwasa, K. H. 1996. Membrane motors in the outer hair cell of the mammalian cochlea. *Comm. Theor. Biol.* 4:93–114.

Iwasa, K. H. 1997. Motor mechanisms of the outer hair cell from the cochlea. *In* Diversity in Auditory Mechanics. E. R. Lewis, G. R. Long, R. F. Lyon, P. M. Narins, and C. R. Steele, editors. World Scientific, Singapore. In press.

Iwasa, K. H., and R. S. Chadwick. 1992. Elasticity and active force generation of cochlear outer hair cells. *J. Acoust. Soc. Am.* 92: 3169–3173.

Iwasa, K. H., and B. Kachar. 1989. Fast in vitro movement of outer hair cells in an external electric field: effect of digitonin, a membrane permeabilizing agent. *Hear. Res.* 40:247–254.

Iwasa, K. H., M. Li, and M. Jia. 1995. Can membrane proteins drive a cell? *Biophys. J.* 68:214S.

Kachar, K., E. B. Brownell, R. Altschuler, and J. Fex. 1986. Electrokinetic shape changes of cochlear outer hair cells. *Nature.* 322:365–367.

Kakehata, S., and J. Santos-Sacchi. 1995. Membrane tension directly shifts voltage dependence of outer hair cell motility and associated gating charge. *Biophys. J.* 68:2190–2197.

Kalinec, E., M. C. Holley, K. H. Iwasa, D. J. Lim, and B. Kachar. 1992. A membrane-based force generation mechanism in auditory sensory cells. *Proc. Natl. Acad. Sci. USA.* 89:8671–8675.

Kojima, H., A. Ishijima, and T. Yanagida. 1994. Direct measurement of stiffness of single actin filaments with and without tropomyosin by in vitro nanomanipulation. *Proc. Natl. Acad. Sci. USA.* 91:12962–12966.

Lieberman, M. C., and L. W. Dodds. 1984. Single neuron labeling and chronic cochlear pathology. III. Stereocilia damage and alterations of threshold tuning curves. *Hear. Res.* 16:55–74.

Mammano, F., and J. F. Ashmore. 1993. Reverse transduction measured in the isolated cochlea by laser Michelson interferometry. *Nature.* 365: 838–841.

Mountain, D. C. 1980. Changes in endolymphatic potential and crossed olivocochlear bundle stimulation alter cochlear mechanics. *Science.* 210: 71–72.

Santos-Sacchi, J. 1991. Reversible inhibition of voltage-dependent outer hair cell motility and capacitance. *J. Neurosci.* 11:3096–3110.

Santos-Sacchi, J., and J. P. Dilger. 1988. Whole cell currents and mechanical responses of isolated outer hair cells. *Hear. Res.* 35:143–150.

Tolomeo, J. A., and C. R. Steele. 1995. Orthotropic piezoelectric properties of the cochlear outer hair cell wall. *J. Acoust. Soc. Am..* 97:3006–3011.

Xue, S., D. C. Mountain, and A. E. Hubbard. 1993. Direct measurement of electrically-evoked basilar membrane motion. *In* Biophysics of Hair Cell Sensory Systems. H. Duifhuis, J. W. Horst, P. van Dijk, P. van Netten, and S. van Netten, editors. World Scientific, Singpore. 361–368.

Zajic, G., and J. Schacht. 1991. Shape changes in isolated outer hair cells: measurements with attached microspheres. *Hear. Res.* 52:407–410.